

# Simultaneous removal of $\text{Cl}^-$ and $\text{SO}_4^{2-}$ from seawater using Mg–Al oxide: kinetics and equilibrium studies

Tomohito Kameda · Jumpei Oba · Toshiaki Yoshioka

Received: 6 January 2014 / Accepted: 14 July 2014 / Published online: 2 August 2014  
© The Author(s) 2014. This article is published with open access at Springerlink.com

**Abstract** Mg–Al oxide, obtained by the thermal decomposition of a  $\text{CO}_3^{2-}$ -intercalated Mg–Al layered double hydroxide ( $\text{CO}_3\cdot\text{Mg–Al}$  LDH), simultaneously absorbed  $\text{Cl}^-$  and  $\text{SO}_4^{2-}$  from seawater and generated a Mg–Al LDH intercalated with  $\text{Cl}^-$  and  $\text{SO}_4^{2-}$ . The Mg–Al oxide with a molar ratio  $\text{Mg}/\text{Al} = 4$  was more superior than the oxide with  $\text{Mg}/\text{Al} = 2$  for  $\text{Cl}^-$  removal, whereas a reverse phenomenon was observed for  $\text{SO}_4^{2-}$  removal. The removal of  $\text{Cl}^-$  and  $\text{SO}_4^{2-}$  by the Mg–Al oxide with  $\text{Mg}/\text{Al} = 4$  could be represented by first-order and pseudo second-order reactions, respectively. The removal of both  $\text{Cl}^-$  and  $\text{SO}_4^{2-}$  by the Mg–Al oxide with  $\text{Mg}/\text{Al} = 2$  could be represented by a pseudo second-order reaction. The removal of both  $\text{Cl}^-$  and  $\text{SO}_4^{2-}$  by the Mg–Al oxides with  $\text{Mg}/\text{Al} = 4$  and 2 was proceeded under chemical reaction control. The adsorption isotherms for  $\text{Cl}^-$  and  $\text{SO}_4^{2-}$  adsorbed by the Mg–Al oxides could be expressed by Langmuir-type adsorption. These reactions were derived from monolayer adsorption, indicating the intercalation of  $\text{Cl}^-$  and  $\text{SO}_4^{2-}$  in the interlayer space of Mg–Al LDH. The uptake of  $\text{Cl}^-$  and  $\text{SO}_4^{2-}$  from seawater by Mg–Al oxide was proceeded spontaneously.

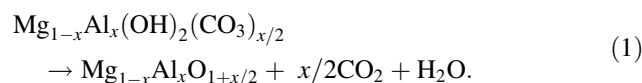
**Keywords** Chloride ion · Sulfate ion · Mg–Al oxide · Simultaneous removal · Kinetics · Equilibrium

## Introduction

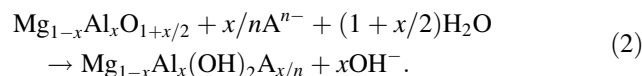
Salt damage can occur in agricultural lands after the incursion of seawater due to typhoons, storm surges, and

tsunamis. It may result from land subsidence, penetration of seawater into groundwater, and leaching of saline from landfill sites. Treatment methods for correcting salt damage include flushing of agricultural land and the dilution of leachate with water. However, these methods require increased water consumption. Therefore, new treatment methods must be developed to remediate environmental salt damage.

Mg–Al layered double hydroxides (Mg–Al LDHs) are well known for their anion-exchange properties (Miyata 1983). Mg–Al LDHs can be represented by the formula  $[\text{Mg}_{1-x}\text{Al}_x^{3+}(\text{OH})_2] (A^{n-})_{x/n}\cdot m\text{H}_2\text{O}$ , where  $x$  denotes the Al/(Mg+Al) molar ratio ( $0.20 \leq x \leq 0.33$ ), and  $A^{n-}$  is an  $n$ -valent anion (Ingram and Taylor 1967; Allmann 1968). The structure of a Mg–Al LDH consists of a stack of Al-bearing, brucite-like octahedral layers, which are positively charged owing to the replacement of some  $\text{Mg}^{2+}$  with  $\text{Al}^{3+}$ , and are electrically neutralized by interlayer anions. The interlayer spaces that are not occupied by anions can contain water molecules. The  $\text{CO}_3^{2-}$ -intercalated Mg–Al LDH ( $\text{CO}_3\cdot\text{Mg–Al}$  LDH) can be converted into Mg–Al oxide by calcination at 450–800 °C:



This Mg–Al oxide can rehydrate and combine with anions to reconstruct the LDH structure:



Mg–Al LDH and Mg–Al oxide have received considerable attention as potential adsorbents for wastewater treatment. Their uptake of contaminants from aqueous solutions has been studied; these include reactive

T. Kameda (✉) · J. Oba · T. Yoshioka  
Graduate School of Environmental Studies, Tohoku University,  
6-6-07 Aoba, Aramaki, Aoba-ku, Sendai 980-8579, Japan  
e-mail: kameda@env.che.tohoku.ac.jp

brilliant orange X-GN, arsenate, arsenite, fluoride, bromate, bromide, selenate, borate, nitrate, and chromate (Chubar 2011; Wu et al. 2011; Lv et al. 2012; Halajnia et al. 2012; Yu et al. 2012). As expressed in Eq. 2, the rehydration and subsequent combination of Mg–Al oxide with anions in solution is accompanied by the release of  $\text{OH}^-$ . Based on this behavior, Mg–Al oxide could both neutralize and fix  $\text{Cl}^-$  in the treatment of HCl (Kameda et al. 2000, 2002, 2005, 2006). Mg–Al oxide was also shown to treat mineral acids such as  $\text{H}_3\text{PO}_4$ ,  $\text{H}_2\text{SO}_4$ , and  $\text{HNO}_3$  (Kameda et al. 2003).

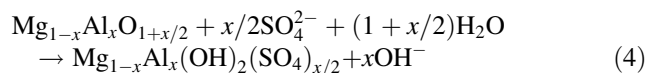
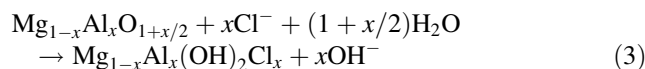
As salt damage is typically derived from the  $\text{Cl}^-$  and  $\text{SO}_4^{2-}$  anions contained in seawater, the absorption capabilities of Mg–Al oxide for those species make it suitable for the treatment of seawater. We propose to spray Mg–Al oxide onto agricultural land as a treatment method for salt damage. In this study, the potential for Mg–Al oxide to absorb  $\text{Cl}^-$  and  $\text{SO}_4^{2-}$  simultaneously from seawater was examined with respect to time, temperature, and quantity of Mg–Al oxide. Kinetics and equilibrium studies on the treatment of seawater by Mg–Al oxide were conducted.

## Materials and methods

All reagents were purchased from Kanto Chemical Co., Inc.  $\text{CO}_3\cdot\text{Mg–Al}$  LDH was prepared by the co-precipitation method. A Mg–Al solution ( $[\text{Mg}^{2+}] + [\text{Al}^{3+}] = 0.5 \text{ M}$ ,  $[\text{Mg}^{2+}]/[\text{Al}^{3+}] = 4.0$  or  $2.0$ ) was prepared by dissolving  $\text{Mg}(\text{NO}_3)_2\cdot 6\text{H}_2\text{O}$  and  $\text{Al}(\text{NO}_3)_3\cdot 9\text{H}_2\text{O}$  in deionized water (500 mL). The Mg–Al solution was added dropwise to  $\text{Na}_2\text{CO}_3$  solution (0.1 or 0.17 M, 500 mL) at 30 °C with mild agitation. The solution pH was adjusted to 10.5 by adding 1.25 M NaOH solution. The mixture was then stirred continuously at 30 °C for 1 h. The  $\text{CO}_3\cdot\text{Mg–Al}$  LDH product was isolated by filtering the resulting suspension, washing it thoroughly with deionized water, and drying under reduced pressure (133 Pa) at 40 °C for 40 h. Mg–Al oxide was then prepared by the thermal decomposition of  $\text{CO}_3\cdot\text{Mg–Al}$  LDH at 500 °C for 2 h. The Mg–Al oxide prepared from the Mg–Al solution with  $[\text{Mg}^{2+}]/[\text{Al}^{3+}] = 4.0$  contained 41.5 wt% Mg and 11.7 wt% Al, resulting in a Mg/Al molar ratio of 3.9. This material was designated Mg–Al oxide (Mg/Al = 4). The Mg–Al oxide prepared from the Mg–Al solution with  $[\text{Mg}^{2+}]/[\text{Al}^{3+}] = 2.0$  contained 20.6 wt% Mg and 11.6 wt% Al, resulting in a Mg/Al molar ratio of 2.0. This material was designated Mg–Al oxide (Mg/Al = 2).

The seawater contained 15,951 mg/L  $\text{Cl}^-$ , 2,265 mg/L  $\text{SO}_4^{2-}$ , 9,893 mg/L  $\text{Na}^+$ , 360 mg/L  $\text{K}^+$ , 1,054 mg/L  $\text{Mg}^{2+}$ , and 310 mg/L  $\text{Ca}^{2+}$ . Seawater (20 mL) and predetermined amounts of the Mg–Al oxides were placed in 50 mL screw-top tubes and shaken at 10–60 °C for 2 min to 7 days. The amounts of the Mg–Al oxides were 0.2 g

and 0.25–5.0 times the stoichiometric quantities indicated by Eqs. 3 and 4:



The suspended solutions were filtered, and the  $\text{Cl}^-$  and  $\text{SO}_4^{2-}$  concentrations of the filtrates were determined using a Dionex DX-120 ion chromatograph and a Dionex model AS-12A column (eluent: 2.7 mM  $\text{Na}_2\text{CO}_3$  and 0.3 mM  $\text{NaHCO}_3$ ; flow rate: 1.3 mL  $\text{min}^{-1}$ ). The products were identified by X-ray diffraction (XRD) analysis using  $\text{Cu K}_\alpha$  radiation.

## Results and discussion

Figure 1 shows the extent of  $\text{Cl}^-$  or  $\text{SO}_4^{2-}$  removal over time at various temperatures for a suspension of Mg–Al oxide (Mg/Al = 4) in seawater. The degree of the  $\text{Cl}^-$  removal increased with time, indicating its uptake from seawater by Mg–Al oxide (Mg/Al = 4), and absorption also increased with increasing temperature. The maximum extent of  $\text{Cl}^-$  removal was 67 % at 60 °C after 360 min. For  $\text{SO}_4^{2-}$ , the percent removal increased with time at 10 and 30 °C, again reflecting the uptake of  $\text{SO}_4^{2-}$  from seawater by Mg–Al oxide (Mg/Al = 4). The removal of  $\text{SO}_4^{2-}$  increased as the temperature rose from 10 to 30 °C, and reached approximately 80 % at both temperatures in 360 min. However, at 60 °C,  $\text{SO}_4^{2-}$  removal increased

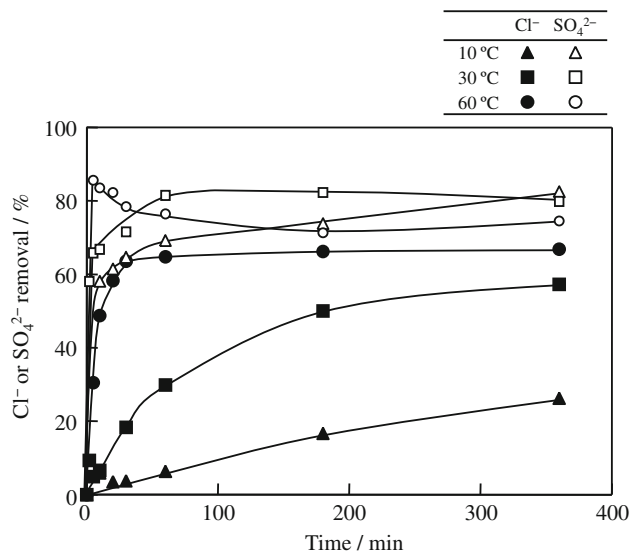


**Fig. 1**  $\text{Cl}^-$  or  $\text{SO}_4^{2-}$  removal versus time during the suspension of Mg–Al oxide (Mg/Al = 4) in seawater at three temperatures. Mg–Al oxide quantity: stoichiometric quantity

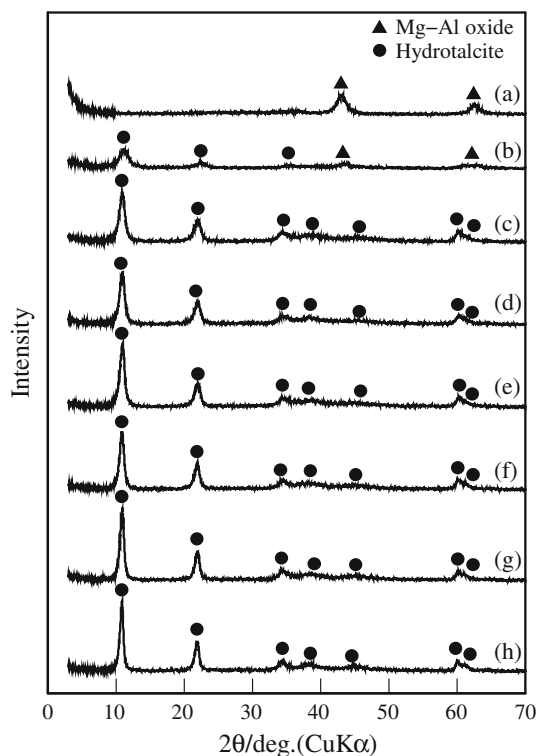


**Fig. 2** XRD patterns for (a) Mg–Al oxide (Mg/Al = 4), and products obtained by the suspension of Mg–Al oxide in seawater at 60 °C for (b) 5, (c) 10, (d) 20, (e) 30, (f) 60, (g) 180, and (h) 360 min. Mg–Al oxide quantity: stoichiometric quantity

rapidly with time, and then decreased. This suggested a desorption of  $\text{SO}_4^{2-}$  after uptake. Since the degree of  $\text{Cl}^-$  removal at 60 °C increased with time, the desorption of  $\text{SO}_4^{2-}$  was probably caused by anion exchange between  $\text{SO}_4^{2-}$  in the interlayer of Mg–Al LDH and  $\text{Cl}^-$  in solution. This indicates that higher temperature promotes the anion exchange, caused by higher concentration of  $\text{Cl}^-$  than  $\text{SO}_4^{2-}$ .

Figure 2 shows the XRD patterns for the Mg–Al oxide (Mg/Al = 4) and the products obtained by its suspension in seawater at 60 °C over several time periods. The XRD peaks ascribed to the Mg–Al oxide disappeared in 10 min, and peaks ascribed to hydrotalcite (JCPDS card 22-700), a naturally occurring hydroxycarbonate of magnesium and aluminum ( $\text{Mg}_6\text{Al}_2(\text{OH})_{16}\text{CO}_3 \cdot 4\text{H}_2\text{O}$ ) with a layered double hydroxide structure, increased with time. This suggested the regeneration of a Mg–Al LDH intercalated with  $\text{Cl}^-$  and  $\text{SO}_4^{2-}$  from the Mg–Al oxide. The  $\text{Cl}^-$  and  $\text{SO}_4^{2-}$  ions were thus removed from seawater by this regenerative process.

Figure 1 showed that the degree of  $\text{Cl}^-$  removal is directly proportional to temperature at any given time. The accelerated rate of  $\text{Cl}^-$  removal at higher temperatures implied that the reaction proceeded under chemical reaction control. Under the assumption that  $\text{Cl}^-$  removal was

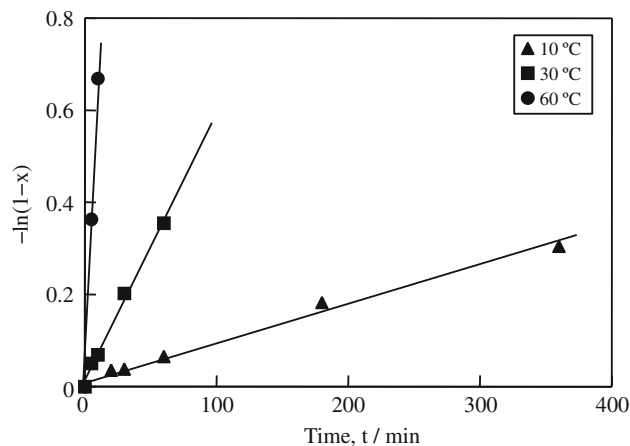


**Fig. 3** First-order plot of  $\text{Cl}^-$  removal by a suspension of Mg–Al oxide (Mg/Al = 4) in seawater at various temperatures. Mg–Al oxide quantity: stoichiometric quantity

governed by first-order kinetics, and using the results shown in Fig. 1, we determined the rate of  $\text{Cl}^-$  removal between 10 and 60 °C according to Eq. 5.

$$-\ln(1-x) = kt, \quad (5)$$

where  $x$  is the degree of  $\text{Cl}^-$  removal,  $t$  is the reaction time, and  $k$  ( $\text{min}^{-1}$ ) is the rate constant for  $\text{Cl}^-$  removal. Figure 3 shows the first-order plots of  $\text{Cl}^-$  removal by a suspension of Mg–Al oxide (Mg/Al = 4) in seawater at various temperatures. The plots showed good linearity at all temperatures, confirming the assumption that  $\text{Cl}^-$  removal could be represented by a first-order reaction. The apparent rate constants at 10, 30, and 60 °C were  $8.3 \times 10^{-4}$ ,  $5.8 \times 10^{-3}$ , and  $6.7 \times 10^{-2} \text{ min}^{-1}$ , respectively. Thus, the apparent rate constant clearly increased with increasing temperature. However, the removal of  $\text{SO}_4^{2-}$  could not be represented by a first-order reaction. Therefore,  $\text{SO}_4^{2-}$  removal was described by pseudo second-order kinetics according to Eq. 6 (Ho and McKay 1999).

$$dq_t/dt = k(q_e - q_t)^2 \quad (6)$$

where  $q_e$  ( $\text{mmol g}^{-1}$ ) is the amount of  $\text{SO}_4^{2-}$  removal at equilibrium,  $q_t$  ( $\text{mmol g}^{-1}$ ) is the amount of  $\text{SO}_4^{2-}$  removal at reaction time,  $t$ , and  $k$  ( $\text{g mmol}^{-1} \text{ min}^{-1}$ ) is the rate constant for  $\text{SO}_4^{2-}$  removal. Integration of Eq. 6 gives

$$t/q_t = 1/(kq_e^2) + t/q_e \quad (7)$$

A first-order reaction postulates a reaction which depends on the concentration of the adsorbate. A pseudo second-order reaction postulates a reaction which is strongly affected by electrostatic interactions between the adsorbent and adsorbate. That is, a pseudo second-order reaction considers the variation of  $\text{SO}_4^{2-}$  concentration in

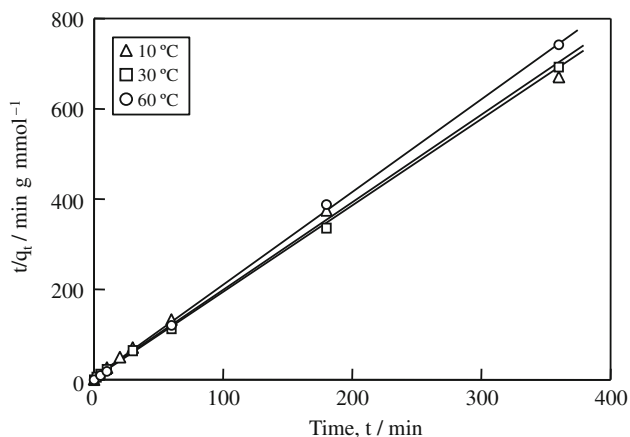


**Fig. 4** Pseudo second-order plot of  $\text{SO}_4^{2-}$  removal by a suspension of Mg–Al oxide (Mg/Al = 4) in seawater at various temperatures. Mg–Al oxide quantity: stoichiometric quantity

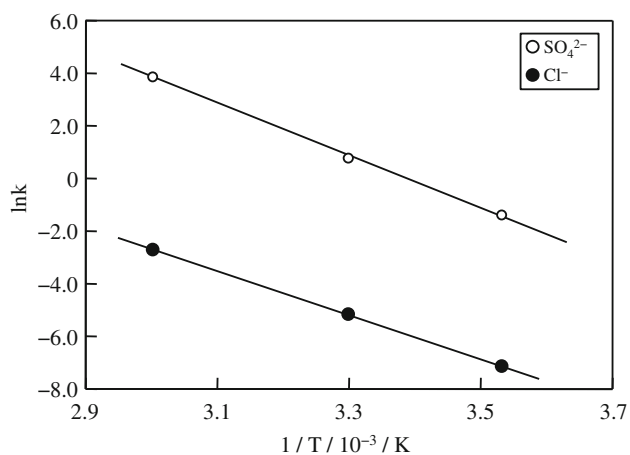


**Fig. 5** Arrhenius plots of the apparent rate constants for  $\text{SO}_4^{2-}$  and  $\text{Cl}^-$  removal by a suspension of Mg–Al oxide (Mg/Al = 4) in seawater. Mg–Al oxide quantity: stoichiometric quantity

the adsorbent and solution. Figure 4 shows pseudo second-order plots for  $\text{SO}_4^{2-}$  removal by a suspension of Mg–Al oxide (Mg/Al = 4) in seawater at various temperatures. The plots show good linearity at all temperatures, confirming that  $\text{SO}_4^{2-}$  removal can be represented by a pseudo second-order reaction. This result may be attributed to the large charge density of  $\text{SO}_4^{2-}$ , which strongly interacts with Mg–Al oxide (Mg/Al = 4). The apparent rate constants at 10, 30, and 60 °C were  $2.5 \times 10^{-1}$ , 2.2, and  $2.0 \times 10^0 \text{ g mmol}^{-1} \text{ min}^{-1}$ , respectively. Thus, the apparent rate constant clearly increased with increasing temperature. Arrhenius plots of  $k$ , determined from the slopes of the lines in Figs. 3 and 4, are shown in Fig. 5; these plots yield apparent activation energies of 68.5 and 68.0  $\text{kJ mol}^{-1}$  for  $\text{Cl}^-$  and  $\text{SO}_4^{2-}$ , respectively. These values confirmed that the removal of  $\text{Cl}^-$  and  $\text{SO}_4^{2-}$  by

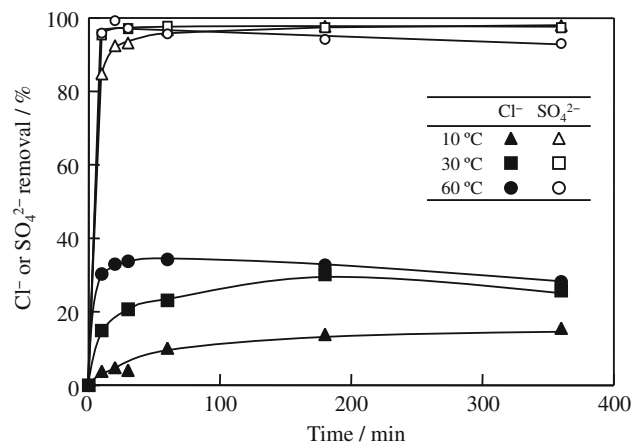
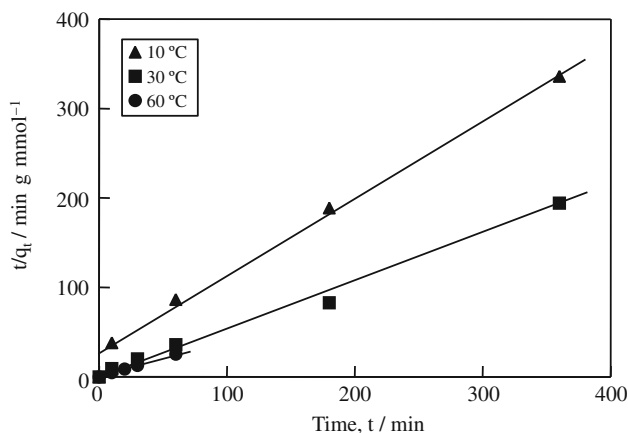


**Fig. 6**  $\text{Cl}^-$  and  $\text{SO}_4^{2-}$  removal versus time during the suspension of Mg–Al oxide (Mg/Al = 2) in seawater at various temperatures. Mg–Al oxide quantity: stoichiometric quantity

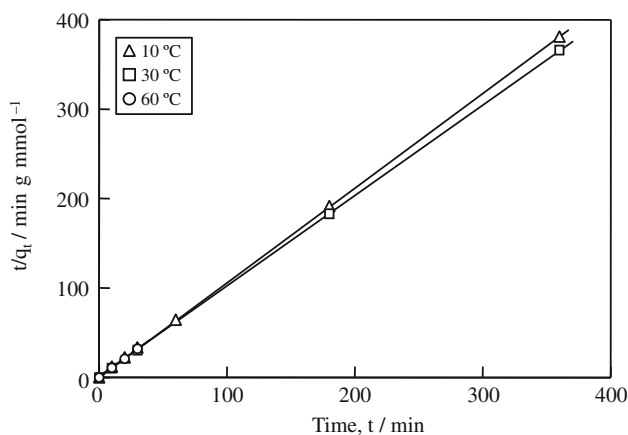
Mg–Al oxide (Mg/Al = 4) proceeded under chemical reaction control.

Figure 6 shows the extent of  $\text{Cl}^-$  or  $\text{SO}_4^{2-}$  removal versus time for a suspension of Mg–Al oxide (Mg/Al = 2) in seawater. Chloride removal increased with time, indicating the uptake of  $\text{Cl}^-$  from seawater by the oxide. The degree of  $\text{Cl}^-$  removal also increased with increasing temperature at all time points.  $\text{Cl}^-$  removal reached a maximum of 34 % at 60 °C and 60 min. The degree of  $\text{SO}_4^{2-}$  removal increased rapidly with time, also indicating the absorption of  $\text{SO}_4^{2-}$  from seawater by Mg–Al oxide (Mg/Al = 2). The degree of  $\text{SO}_4^{2-}$  removal increased with increasing temperature, and the maximum absorption was 99 % at 60 °C after 20 min. By comparing Figs. 1 and 6,  $\text{Cl}^-$  removal by Mg–Al oxide (Mg/Al = 4) was higher than that by Mg–Al oxide (Mg/Al = 2), whereas the reverse capability was observed for  $\text{SO}_4^{2-}$  removal. Therefore, a magnesium/aluminum ratio of four was superior for  $\text{Cl}^-$  removal, and a magnesium/aluminum ratio of two was superior for  $\text{SO}_4^{2-}$  removal.

Figure 6 shows the degree of  $\text{Cl}^-$  removal directly proportional to temperature at any time. The accelerated rate of  $\text{Cl}^-$  removal at higher temperatures implied that the reaction proceeded under chemical reaction control. However,  $\text{Cl}^-$  removal could not be represented by a first-order reaction. Therefore,  $\text{Cl}^-$  removal was described by pseudo second-order kinetics according to Eq. 6. Figure 7 displays pseudo second-order plots of  $\text{Cl}^-$  removal by the suspension of Mg–Al oxide (Mg/Al = 2) in seawater at various temperatures. The plots showed good linearity at all temperatures, confirming that  $\text{Cl}^-$  removal could be represented by a pseudo second-order reaction. The apparent rate constants clearly increased with increasing temperature, with values of  $3.6 \times 10^{-2}$ ,  $1.5 \times 10^{-1}$ , and  $4.8 \times 10^{-1} \text{ g mmol}^{-1} \text{ min}^{-1}$  at 10, 30, and 60 °C,



**Fig. 7** Pseudo second-order plots of  $\text{Cl}^-$  removal by a suspension of Mg–Al oxide (Mg/Al = 2) in seawater at various temperatures. Mg–Al oxide quantity: stoichiometric quantity



**Fig. 8** Pseudo second-order plots of  $\text{SO}_4^{2-}$  removal by a suspension of Mg–Al oxide (Mg/Al = 2) in seawater at various temperatures. Mg–Al oxide quantity: stoichiometric quantity

respectively. Similarly,  $\text{SO}_4^{2-}$  removal by Mg–Al oxide (Mg/Al = 2) could not be described by a first-order reaction. Therefore, the  $\text{SO}_4^{2-}$  removal was also represented by pseudo second-order kinetics according to Eq. 6. Pseudo second-order plots of  $\text{SO}_4^{2-}$  removal by the suspension of Mg–Al oxide (Mg/Al = 2) in seawater at various temperatures are presented in Fig. 8. The good linearity of the plots at all temperatures confirmed the validity of the pseudo second-order representation for  $\text{SO}_4^{2-}$  removal. The apparent rate constants clearly increased with increasing temperature, with values of  $7.7 \times 10^{-1}$ , 3.9, and  $3.7 \times 10 \text{ g mmol}^{-1} \text{ min}^{-1}$  at 10, 30, and 60 °C, respectively. Arrhenius plots of  $k$ , determined from the slopes of the lines in Figs. 7 and 8, are shown in Fig. 9; these plots yield apparent activation energies of 40.2 and  $60.8 \text{ kJ mol}^{-1}$  for  $\text{Cl}^-$  and  $\text{SO}_4^{2-}$ , respectively. These values confirmed that the removal of  $\text{Cl}^-$  and  $\text{SO}_4^{2-}$  by

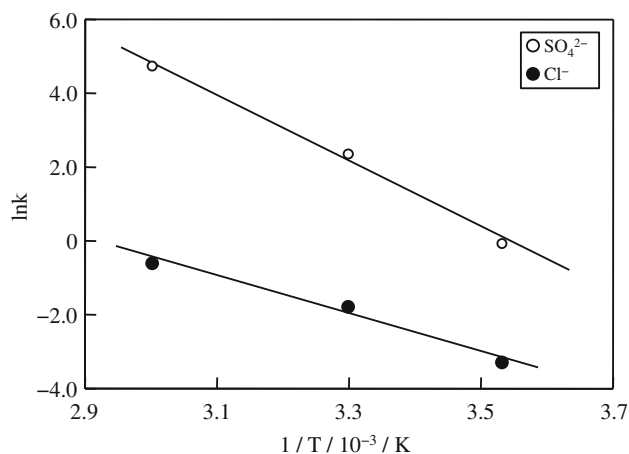


**Fig. 9** Arrhenius plots of the apparent rate constants for  $\text{SO}_4^{2-}$  and  $\text{Cl}^-$  removal by the suspension of Mg–Al oxide (Mg/Al = 2) in seawater. Mg–Al oxide quantity: stoichiometric quantity

Mg–Al oxide (Mg/Al = 2) proceeded under chemical reaction control.

Figure 10 shows the effect of Mg–Al oxide loading on the degree of  $\text{Cl}^-$  or  $\text{SO}_4^{2-}$  removal after the suspension of Mg–Al oxide in seawater at 30 °C for 24 h. For both Mg–Al molar ratios, the extent of  $\text{Cl}^-$  and  $\text{SO}_4^{2-}$  removal increased with increasing Mg–Al oxide quantity. For the Mg–Al oxide loadings between 0.25 and 1.25 molar equivalents, Mg–Al oxide (Mg/Al = 4) was superior to Mg–Al oxide (Mg/Al = 2) for  $\text{Cl}^-$  removal, whereas the opposite was true for  $\text{SO}_4^{2-}$  removal, as mentioned above. For Mg–Al oxide amounts above 2.0 molar equivalents, the removal of  $\text{Cl}^-$  and  $\text{SO}_4^{2-}$  for Mg–Al oxide (Mg/Al = 4) and of  $\text{SO}_4^{2-}$  for Mg–Al oxide (Mg/Al = 2) were over 90 %. However, the  $\text{Cl}^-$  removal for Mg–Al oxide (Mg/Al = 2) was only 55 % at quantity loading of 4.0 molar equivalents. The decrease in the Mg/Al molar ratio would have caused an increase in the positive charge of the host layers in the reconstructed Mg–Al LDH (Sato et al. 1987), and  $\text{OH}^-$  ions, with a charge density greater than that of  $\text{Cl}^-$ , would presumably have intercalated within the interlayer to compensate for the increased positive charge (Kameda et al. 2006). Figures 7 and 8 showed that  $\text{Cl}^-$  and  $\text{SO}_4^{2-}$  removal by Mg–Al oxide (Mg/Al = 2) could be represented by a pseudo second-order reaction, which was attributed to the large positive charge of the host layers for the reconstructed Mg–Al LDH (Mg/Al = 2), which strongly interacted with  $\text{Cl}^-$  and  $\text{SO}_4^{2-}$ . Furthermore, Figs. 5 and 9 showed that the apparent activation energies for  $\text{Cl}^-$  and  $\text{SO}_4^{2-}$  removal by Mg–Al oxide (Mg/Al = 2) were lower than those by Mg–Al oxide (Mg/Al = 4), which was attributed to the larger electrostatic interaction between the adsorbent and adsorbate for Mg/Al = 2 than Mg/Al = 4.

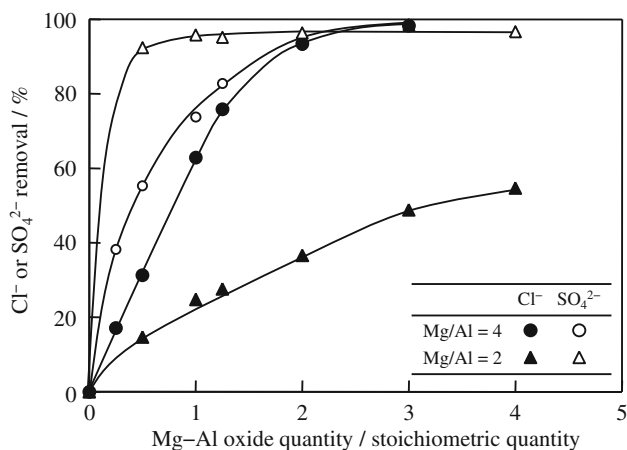


**Fig. 10** Effect of Mg–Al oxide quantity on  $\text{Cl}^-$  and  $\text{SO}_4^{2-}$  removal during the suspension of Mg–Al oxide in seawater at 30 °C for 24 h

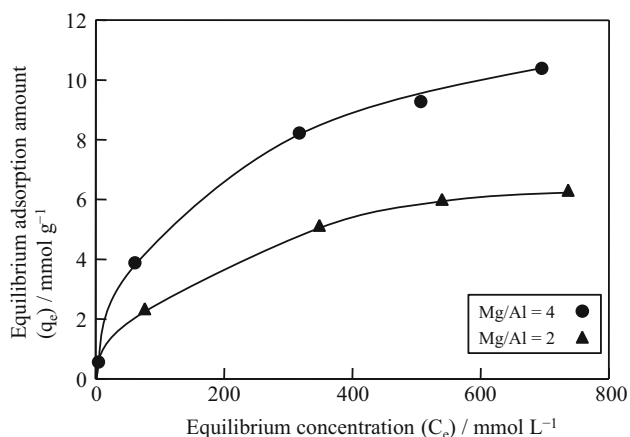


**Fig. 11** Adsorption isotherms of  $\text{Cl}^-$  adsorption by Mg–Al oxides. Mg–Al oxide quantity: 0.2 g; Initial NaCl concentration: 0.01–0.8 M; Temperature: 30 °C; Time: 7 days

Figure 11 shows the adsorption isotherms for  $\text{Cl}^-$  adsorption by the Mg–Al oxides. For both Mg/Al molar ratios, the equilibrium adsorption amount increased with increasing equilibrium concentration. The curves were considered to be Langmuir-type adsorption isotherms. This hypothesis was confirmed by arranging the experimental data according to the Langmuir equation, which can be expressed as

$$q_e = C_e q_m K_L / (1 + C_e K_L), \quad (8)$$

where  $q_e$  ( $\text{mmol g}^{-1}$ ) is the equilibrium adsorption amount,  $C_e$  ( $\text{mmol L}^{-1}$ ) is the equilibrium concentration,  $q_m$  ( $\text{mmol g}^{-1}$ ) is the maximum adsorption amount, and  $K_L$  is the equilibrium adsorption constant. Equation 8 can be converted to Eq. 9:

$$C_e/q_e = 1/q_m K_L + C_e/q_m. \quad (9)$$

Figure 12 shows  $C_e/q_e$  versus  $C_e$  plots for the adsorption isotherms of  $\text{Cl}^-$  adsorbed by the Mg–Al oxides. Good

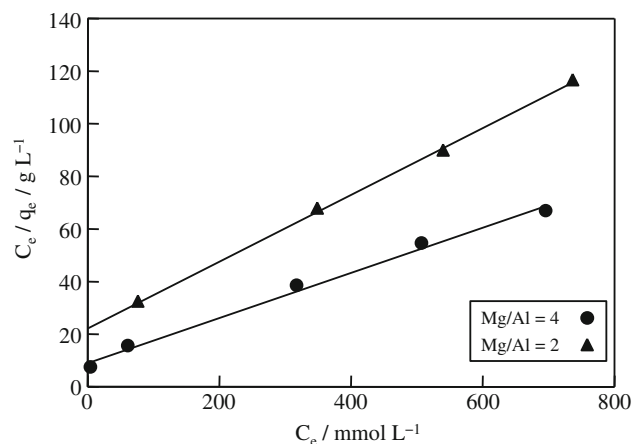


**Fig. 12**  $C_e/q_e$  versus  $C_e$  plots for the adsorption isotherms of  $\text{Cl}^-$  adsorbed by Mg–Al oxides. Mg–Al oxide quantity: 0.2 g; Initial NaCl concentration: 0.01–0.8 M; Temperature: 30 °C; Time: 7 days

linearity was obtained, indicating that this reaction can be expressed as a Langmuir-type adsorption. The reaction results from monolayer adsorption, an intercalation of  $\text{Cl}^-$  in the interlayer space of the Mg–Al LDH. The values of  $q_m$  and  $K_L$ , determined from the slopes and intercepts of the lines in Fig. 12, were 11.7  $\text{mmol g}^{-1}$  and 8.9 for Mg/Al = 4, and 7.9  $\text{mmol g}^{-1}$  and 5.5 for Mg/Al = 2, respectively. The Gibbs free energy change ( $\Delta G$ ) for  $\text{Cl}^-$  removal was estimated by the following equation:

$$\Delta G = -RT \ln K_L, \quad (10)$$

where  $R$  is the gas constant, 8.314  $\text{J K}^{-1} \text{mol}^{-1}$ , and  $T$  (K) is absolute temperature.  $\Delta G$  values were calculated to be  $-5.5$  and  $-4.3$   $\text{kJ mol}^{-1}$  for Mg/Al = 4 and 2, respectively. Thus, the uptake of  $\text{Cl}^-$  from seawater by the Mg–Al oxides proceeded spontaneously.

The adsorption isotherms for the absorption of  $\text{SO}_4^{2-}$  by the Mg–Al oxides are shown in Fig. 13. For both Mg/Al molar ratios, the equilibrium adsorption amount increased with increasing equilibrium concentration. These curves are also considered to be Langmuir-type adsorption isotherms, which was similarly confirmed by arranging the experimental data according to the Langmuir equation. Figure 14 displays  $C_e/q_e$  versus  $C_e$  plots for the adsorption isotherms of  $\text{SO}_4^{2-}$  adsorbed by the Mg–Al oxides. Again, good linearity was obtained, which indicated that this reaction could be expressed as a Langmuir-type adsorption. This reaction is derived from monolayer adsorption, indicating the intercalation of  $\text{SO}_4^{2-}$  in the interlayer space of the Mg–Al LDH. The values of  $q_m$  and  $K_L$ , determined from the slopes and intercepts of the lines in Fig. 14, were 1.8  $\text{mmol g}^{-1}$  and  $6.2 \times 10^3$  for Mg/Al = 4, and 2.0  $\text{mmol g}^{-1}$  and  $6.0 \times 10^2$  for Mg/Al = 2, respectively.  $\Delta G$  values for  $\text{SO}_4^{2-}$  were calculated to be  $-22$  and  $-16$   $\text{kJ mol}^{-1}$  for Mg/Al = 4 and 2, respectively. Thus, the

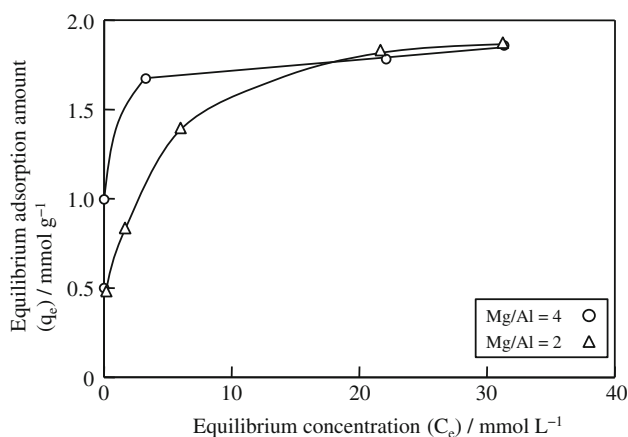


**Fig. 13** Adsorption isotherms of  $\text{SO}_4^{2-}$  adsorption by Mg–Al oxides. Mg–Al oxide quantity: 0.2 g; Initial  $\text{Na}_2\text{SO}_4$  concentration: 0.005–0.05 M; Temperature: 30 °C; Time: 7 days

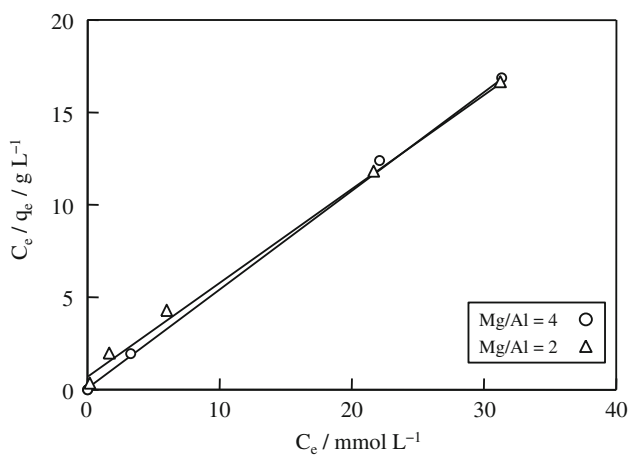


**Fig. 14**  $C_e/q_e$  versus  $C_e$  plots for the adsorption isotherms of  $\text{SO}_4^{2-}$  adsorbed by Mg–Al oxides. Mg–Al oxide quantity: 0.2 g; Initial  $\text{Na}_2\text{SO}_4$  concentration: 0.005–0.05 M; Temperature: 30 °C; Time: 7 days

uptake of  $\text{SO}_4^{2-}$  from seawater by the Mg–Al oxides also proceeded spontaneously.

## Conclusion

The Mg–Al oxides simultaneously absorbed  $\text{Cl}^-$  and  $\text{SO}_4^{2-}$  from seawater, in a process that generated a Mg–Al LDH intercalated with  $\text{Cl}^-$  and  $\text{SO}_4^{2-}$ . Mg–Al oxide (Mg/Al = 4) was superior to Mg–Al oxide (Mg/Al = 2) for  $\text{Cl}^-$  removal, and whereas the reverse capability was observed for  $\text{SO}_4^{2-}$  removal. Chloride removal by Mg–Al oxide (Mg/Al = 4) could be represented by a first-order reaction, however, sulfate removal over the same substrate required a pseudo second-order reaction representation. The apparent activation energies were 68.5 and

68.0  $\text{kJ mol}^{-1}$  for  $\text{Cl}^-$  and  $\text{SO}_4^{2-}$  removal by Mg–Al oxide (Mg/Al = 4), respectively, confirming that these processes proceeded under chemical reaction control. The removal of both  $\text{Cl}^-$  and  $\text{SO}_4^{2-}$  by Mg–Al oxide (Mg/Al = 2) could be represented by pseudo second-order reactions. Here, the apparent activation energies were 40.2 and 60.8  $\text{kJ mol}^{-1}$  for  $\text{Cl}^-$  and  $\text{SO}_4^{2-}$ , respectively, also indicating processes under chemical reaction control. Furthermore, the adsorption isotherms for  $\text{Cl}^-$  and  $\text{SO}_4^{2-}$  adsorbed by the Mg–Al oxides could be expressed by Langmuir-type adsorptions. This reaction is derived from monolayer adsorption, indicating the intercalation of  $\text{Cl}^-$  and  $\text{SO}_4^{2-}$  in the interlayer space of the Mg–Al LDH. For  $\text{Cl}^-$ , the maximum adsorption amount and equilibrium adsorption constant were 11.7  $\text{mmol g}^{-1}$  and 8.9 for Mg/Al = 4, and 7.9  $\text{mmol g}^{-1}$  and 5.5 for Mg/Al = 2, respectively. The Gibbs free energy changes for  $\text{Cl}^-$  removal were  $-5.5$  and  $-4.3$   $\text{kJ mol}^{-1}$  for Mg/Al = 4 and 2, respectively. The uptake of  $\text{Cl}^-$  from seawater by Mg–Al oxide proceeded spontaneously. For  $\text{SO}_4^{2-}$ , the maximum adsorption amount and equilibrium adsorption constant were 1.8  $\text{mmol g}^{-1}$  and  $6.2 \times 10^3$  for Mg/Al = 4, and 2.0  $\text{mmol g}^{-1}$  and  $6.0 \times 10^2$  for Mg/Al = 2, respectively. The Gibbs free energy changes for  $\text{SO}_4^{2-}$  were  $-22$  and  $-16$   $\text{kJ mol}^{-1}$  for Mg/Al = 4 and 2, respectively. The uptake of  $\text{SO}_4^{2-}$  from seawater by Mg–Al oxide also proceeded spontaneously.

**Open Access** This article is distributed under the terms of the Creative Commons Attribution License which permits any use, distribution, and reproduction in any medium, provided the original author(s) and the source are credited.

## References

- Allmann R (1968) The crystal structure of pyroaurite. *Acta Crystallogr B* 24:972–977
- Chubar N (2011) New inorganic (an)ion exchangers based on Mg–Al hydrous oxides: (Alkoxide-free) sol-gel synthesis and characterization. *J Colloid Interface Sci* 357:198–209
- Halajnia A, Oustan S, Najafi N, Khataee AR, Lakzian A (2012) The adsorption characteristics of nitrate on Mg–Fe and Mg–Al layered double hydroxides in a simulated soil solution. *Appl Clay Sci* 70:28–36
- Ho YS, McKay G (1999) Pseudo-second order model for sorption processes. *Process Biochem* 34:451–465
- Ingram L, Taylor HFW (1967) The crystal structures of sjogrenite and pyroaurite. *Miner Mag* 36:465–479
- Kameda T, Miyano Y, Yoshioka T, Uchida M, Okuwaki A (2000) New treatment methods for waste water containing chloride ion using magnesium–aluminum oxide. *Chem Lett* 29:1136–1137
- Kameda T, Yoshioka T, Uchida M, Miyano Y, Okuwaki A (2002) New treatment method for dilute hydrochloric acid using magnesium–aluminum oxide. *Bull Chem Soc Jpn* 75:595–599
- Kameda T, Yabuuchi F, Yoshioka T, Uchida M, Okuwaki A (2003) New method of treating dilute mineral acids using magnesium–aluminum oxide. *Wat Res* 37:1545–1550

- Kameda T, Yoshioka T, Hoshi T, Uchida M, Okuwaki A (2005) The removal of chloride from solutions with various cations using magnesium-aluminum oxide. *Sep Purif Tech* 42:25–29
- Kameda T, Yoshioka T, Hoshi T, Uchida M, Okuwaki A (2006) Treatment of hydrochloric acid with magnesium-aluminum oxide at ambient temperatures. *Sep Purif Tech* 51:272–276
- Lv T, Ma W, Xin G, Wang R, Xu J, Liu D, Liu F, Pan D (2012) Physicochemical characterization and sorption behavior of Mg-Ca-Al ( $\text{NO}_3$ ) hydrotalcite-like compounds toward removal of fluoride from protein solutions. *J Hazard Mater* 237–238:121–132
- Miyata S (1983) Anion-exchange properties of hydrotalcite-like compounds. *Clays Clay Miner* 31:305–311
- Sato T, Tezuka M, Endo T, Shimada M (1987) Kinetics of anion uptake by rock salt-type magnesium aluminum oxide solid solutions. *React Solids* 3:287–295
- Wu P, Zhang Q, Dai Y, Zhu N, Li P, Wu J, Dang Z (2011) Removal of reactive brilliant orange X-GN from aqueous solutions by Mg-Al layered double hydroxides. *Clays Clay Miner* 59:438–445
- Yu XY, Luo T, Jia Y, Xu RX, Gao C, Zhang YX, Liu JH, Huang XJ (2012) Three-dimensional hierarchical flower-like Mg-Al-layered double hydroxides: highly efficient adsorbents for As(V) and Cr(VI) removal. *Nanoscale* 4:3466–3474